Improvements in time resolution of tomographic photoacoustic imaging using a priori information for multiplexed systems

John Gamelin, Andres Aguirre, Anastasios Maurudis, Lihong V. Wang, Quing Zhu

John Gamelin, Andres Aguirre, Anastasios Maurudis, Lihong V. Wang, Quing Zhu, "Improvements in time resolution of tomographic photoacoustic imaging using a priori information for multiplexed systems," Proc. SPIE 7177, Photons Plus Ultrasound: Imaging and Sensing 2009, 71771C (24 February 2009); doi: 10.1117/12.813558

SPIE.

Event: SPIE BiOS, 2009, San Jose, California, United States

Improvements in Time Resolution of Tomographic Photoacoustic Imaging using *A Priori* Information for Multiplexed Systems

John Gamelin, Andres Aguirre, Anastasios Maurudis, Lihong V. Wang*, and Quing Zhu

University of Connecticut, Biomedical Ultrasound and Optical Imaging Group, Storrs, CT 06269
* Washington University in St. Louis, Dept. of Biomedical Engineering, St. Louis, MO 63130-4899

ABSTRACT

We present results of investigations of the application of *a priori* information and sparse or limited-view algorithms to simultaneously improve imaging quality and time-resolution in photoacoustic tomography. Modified versions of existing MRI/CT algorithms such as constrained backprojection and keyhole imaging are evaluated as well as a new Wiener estimation methods for extrapolation of missing data from reference data sets. Simulations indicate the effectiveness of the approaches for accurate tracking of dynamic photoacoustic events for data sets with limited views (< 90 degrees) or tomographic views with up to 1/64 of the full data set. We present experimental data of contrast uptake and washout using a 512-element curved transducer with 1:8 electronic multiplexing that demonstrates high-resolution tomographic imaging with a temporal resolution of better than 150 milliseconds using these methods.

Keywords: Photoacoustic tomography, real-time imaging, reconstruction, backprojection

1. INTRODUCTION

One of the promises of photoacoustic tomography is the potential for real-time functional imaging of optical contrast. For example, the response to trauma, blood flow and oxygen saturation changes accompanying physiological stimulus, or the dynamic uptake of a targeted contrast agent could be monitored with the video-rate time response characteristic of ultrasound imaging. Other optical techniques appropriate for deep-tissue imaging, such as Diffusive Optical Tomography (DOT), generally require complex inverse reconstruction techniques that preclude instantaneous image results or involve scanning that can limit time resolution to the order of seconds with post-acquisition processing.

Although the potential for fast imaging exists, the time resolution of tomographic photoacoustic systems is usually limited to the repetition rate of the laser, typically less than 20 Hz. Further constraints on the imaging frame rate can be introduced by the practical need for electronic multiplexing in the acquisition for systems with large

Photons Plus Ultrasound: Imaging and Sensing 2009, edited by Alexander A. Oraevsky, Lihong V. Wang,
Proc. of SPIE Vol. 7177, 71771C · © 2009 SPIE · CCC code: 1605-7422/09/$18 · doi: 10.1117/12.813558

numbers of transducer elements as may be dictated by cost, size, or complexity constraints. Smaller numbers of elements, or limited views, can be used to enable real-time monitoring of photoacoustic events, but only at the expense of reduced spatial resolution or imaging quality due to limited data set considerations. For well-established imaging modalities, such as CT and MRI, sparse data algorithms have been developed that enable three-dimensional time-resolved imaging for monitoring of dynamic events such as contrast agent uptake or limit radiation dosage to the patient[1-5].

In this paper, we present techniques for improving the time resolution of photoacoustic systems for which complete imaging data is not available at each acquisition time. This limitation is routinely encountered for systems with multiplexed receiver electronics or systems employing mechanical scanning of transducers. Application of the algorithms, which take advantage of high quality reference scans generated prior to or during the imaging sequence, improve spatial resolution and feature definition while preserving much of the transient dynamics of the process. After introduction of the methodologies, we present results of simulation, phantom, and in vivo imaging studies demonstrating the effectiveness and limitations of the approaches.

2. ALGORITHMS

Introduction

Established whole-body imaging modalities such as CT and MRI typically require mechanical scanning of the source and detector apparatus to generate images of single anatomical slices or volumes. Capture of dynamic events such as flow and uptake of contrast agents present challenges due to the comparatively long times required for acquisition of a fully sampled sequence to minimize artifacts and maintain high spatial resolution. In addition, increased radiation exposure during the imaging of an uptake session represents a health concern for patients. For these reasons, several techniques for limiting the number of views or projections during dynamic and 3D imaging sessions have been investigated for CT and MRI [1-5]. The differences of the photoacoustic imaging model necessitate modification of the previous approaches for conventional modalities and motivate development of new algorithms tailored for the pressure/time-based data sets for photoacoustic.

In a typical photoacoustic tomographic geometry, pressure data from transducer elements placed on the circumference of a closed, two-dimensional measurement surface is used to generate a high-resolution image of a target absorption profile. If data from portions of the closed surface are not available at any given time, artifacts such as streaking and bowing are generated due to the limited view. The extent of artifacts is highly dependent upon the distribution of the active transducer elements and the position and geometry of the feature of interest [6].

In the absence of current data for the missing elements, we propose the use of *a priori* information, generated during a complete scan acquired prior to or during the imaging sequence, to reduce the impact of artifacts. Two general approaches for improving the image quality are considered here. One method is to use data from the limited set of

elements active at an instant of time and use the *a priori* reference data to constrain or weight the current data spatially and temporally. The highly constrained back-projection technique introduced by Mistretta et. al. [5] has been successfully applied to MRI and will be evaluated for the effectiveness with photoacoustic data. The second class of approaches relies upon augmenting or expanding the set of current data with estimates of the data that would have been acquired for the missing elements. A variation on the keyhole technique [3], also used for MRI, is investigated here. In addition, we propose a new Wiener estimation method for construction of approximate data for non-active elements using data from the active transducers.

Limited Data Sets: Constrained Backprojection

The highly constrained backprojection method involves normalization and weighting of projections from a complete reference data to improve time resolution while preserving spatial resolution. In this technique, circular projections representing the summed pressure originating from points a fixed distance from the active elements are normalized to the corresponding projections of the same elements from the reference data set. The normalized projections are then summed for each point within the imaging region as in traditional backprojection algorithms and divided by the number of contributing projections for the given time instant. The resulting image is weighted by the reference imaging formed from the complete reference data set:

$$I(r,t) = \frac{I_{ref}(r)}{N_{pr}} \sum_{j=1}^{N_{pr}} \left. \frac{P^{j}{}_{cur}(t',t)}{P^{j}{}_{ref}(t')} \right|_{t'=\frac{r-r_j}{c}} \tag{1.1}$$

In this equation I(r) is the image, Npr is the number of contributing projections (j) at the current time instant, and P(t) is the projection corresponding to retarded time t'.

Mistretta et. al. [5]have demonstrated that the signal-to-noise ratio (SNR) for this method is determined primarily by the SNR of the reference data set. Because this reference data can be acquired with significant averaging, demonstrable improvement in imaging quality can be achieved.

Augmented Data Sets: Keyhole and Wiener Estimation

An alternative approach to improving time resolution relies upon expanding the limited data set with information obtained from the reference set. For situations with limited undersampling (e.g. factor of 2), sparse absorption distributions, or small changes in the targets, the keyhole technique [3] may be appropriate. As the name suggests, this approach assumes that one has a limited view on current data ("through the keyhole") and that one can complete the picture by using reference data ("the lock"). In MRI, this technique used reference k-space information whereas here we use projection data.

Another method for completing the data set is to not use the reference data itself, but instead use the relationships between active and inactive elements in the reference frame to estimate the data that would be acquired from inactive elements at the time instant using the data from the current active elements. Figure 1 depicts a heuristic representation of the estimation procedure. The signal received at a given transducer

element following a photoacoustic excitation of a target reflects the spatio-temporal propagation of the generated photoacoustic signal. From a linear systems perspective, the detected signal can be represented in the time-based frequency domain by a transfer function (F(ω) and G(ω) for elements A and B, respectively) of the photoacoustic source signal. One can form an effective transfer function relating the signals received by the two elements, H(ω), that accounts for deconvolution of the forward propagation from element A to the source followed by convolution of the forward propagation from the source to element B. Assuming that this relationship between the two detected signals obtained in the reference frame approximately applies to the current time instant (i.e. small perturbations), the transfer function can predict the response for any unknown element B given the detected signal from element A.

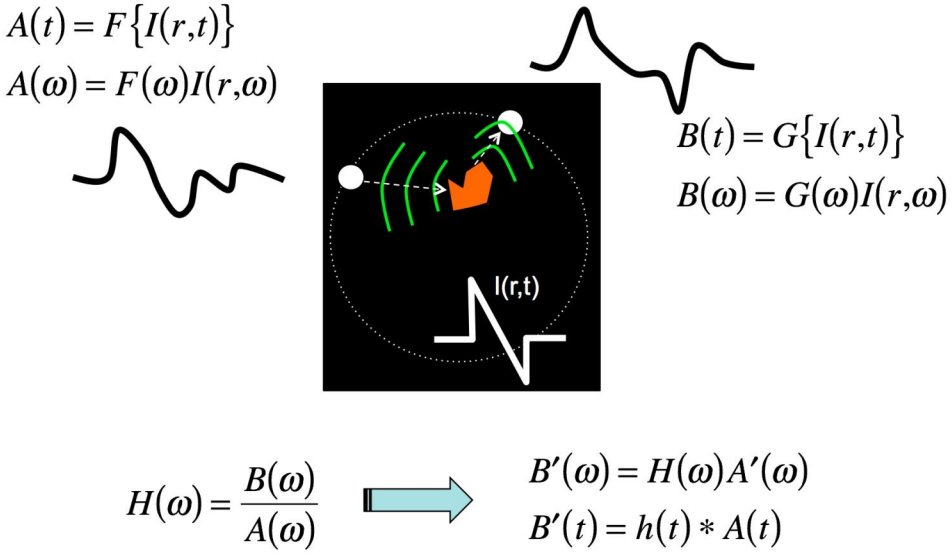

Figure 1. Heuristic depiction of Wiener estimation principle.

In practice, noise and uncertainties can make the deconvolution subject to sensitivities division of spectral components with low value. In order to reduce the potential impact of these effects, a Wiener deconvolution technique [7] has been employed to account for system noise contributions. The estimated signal for an inactive element B at time instant t is calculated from the response of an active element A using

$$\tilde{p}_B(t) = \Im^{-1}\left\{ P_A^{\ t}(\omega) \frac{P_B^{\ ref}(\omega)}{P_A^{\ ref}(\omega)\left[1 + \left\| \frac{N_A(\omega)}{P_A^{\ ref}(\omega)} \right\|^2\right]} \right\} \tag{1.2}$$

In this equation, $\tilde{p}_B(t)$ is the estimated pressure at time t for inactive element B, $\Im^{-1}$ is the inverse Fourier Transform, $P_{A,B}(\omega)$ are the Fourier transforms of the detected pressures for elements A and B, respectively, and $N_A(\omega)$ is the measured electronic noise spectrum for element A. The bracketed term accounts for the SNR by attenuating the transfer function for low SNR values. For implementation, the maximum spectral amplification, given by the multiplicative term to $P_A^{\,t}(\omega)$, is limited to 5 or 20 for further robustness.

3. SIMULATION STUDIES

To evaluate the effectiveness and limitations of the algorithms, simulations were performed. The first numerical phantom consisted of three spheres with diameters ranging from 3 to 10 mm. The two smaller spheres were modulated anti-phase with modulation depths of 50% while the larger sphere was kept constant (Table 1). The reference frame was chosen to coincide with the average value throughout an eight-interval time period. Uncorrelated white Gaussian noise with an amplitude 10% of the peak detected signal was added independently to each element for both the reference and time-varying data set. The analytic photoacoustic formula from Diebold et. al. [8] was used for generation of the detected signals.

Table 1. Analytic spheres numerical phantom parameters.

Target	Center Location (mm)	Diameter (mm)	Absorption (AU)
S1	(-5,-5)	3	$1+0.5\sin\left(\frac{2\pi\, firing}{8}\right)$
S2	(0,0)	10	0.5
S3	(10,10)	5	$0.25\times\left[1-0.5\sin\left(\frac{2\pi\, firing}{8}\right)\right]$

The complete measurement aperture was selected to model a tomographic small animal imaging system developed in our lab [9]. The system comprises 512 elements distributed along a circular boundary with 50 mm diameter. The multiplexing scheme requires eight acquisitions for a complete data set. For any given firing, more than 50% of the aperture is not sampled and the overall undersampling factor is eight.

Figure 2 depicts the time variations of the mean values for each of the targets. With the exception of the keyhole technique, which in this case consists of 85% reference signal content, the sinusoidal variation of the modulated absorption values is preserved.

Because of the large modulation depth, changes in the highest absorber (target 1) reduce the estimated swings for the antiphase absorber (target 3). The images of the static sphere preserve the expected nearly constant value. In this particular case, the strong modulation of the high absorber produced corresponding variations in the static absorber for the constrained backprojection method along with a net positive bias with respect to the true value. All of the algorithms considered herein assume small changes in heterogeneity with respect to the reference distribution so that large variations result in crosstalk to nearby targets for which the photoacoustic signals overlap in time.

In order to investigate more realistic and complex geometries, a second numerical phantom consisting of rectangular and elliptical structures was constructed. A two-dimensional Fourier Transform forward model [10] generated the reference and time-varying received data and a two-dimensional backprojection algorithm was used for reconstruction [11]. One each of the elliptical and rectangular structures was increased in an exponential fashion to mimic uptake of a contrast agent while the other two structures were held fixed. The reference configuration was chosen to reflect the t=0 values and the transducer element pattern over the time course of eight time samples was the multiplexed ring transducer pattern.

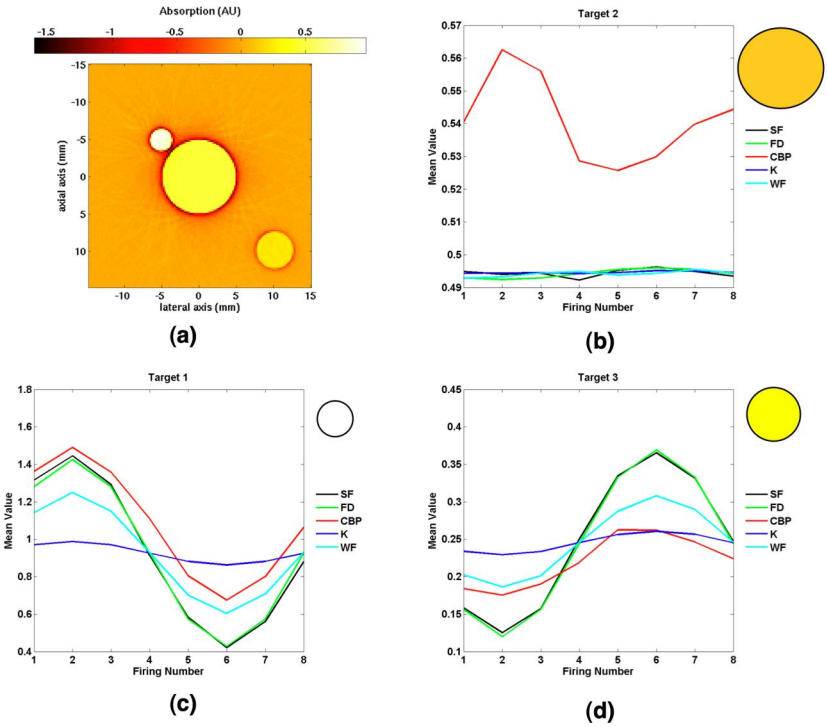

Figure 2. Mean values for targets with the 3-sphere digital phantom.

Table 2. Target parameters for two-dimensional ellipse-square numerical phantom.

Target	Center Location (x,y) mm	Elliptical Axis Lengths (mm)	Rotation Angle (degrees)	Absorption (AU)
3	(4.75,0)	(5.3,1.9)	72	0.1
4	(-5.95,0)	(3.4,3.4)	108	$0.15\left[2-e^{\frac{-firing}{4}}\right]$
5	(0,-4.25)	(0.85,8.5)	90	$0.20\left[2-e^{\frac{-firing}{4}}\right]$
6	(0,8.5)	(5.95,1.7)	0	0.3

Figure 3 depicts the reconstructed images using the single-acquisition data without a priori information along with the corresponding images for the three algorithms. Without a priori information, severe artifacts and streaking is observed whereas all the techniques considering reference information faithfully reproduce the features with high definition and quantitative accuracy. To test the limits of the techniques, simulations were performed for undersampling ratios of 8 to 64 assuming a uniform angular distribution around the circular measurement surface. Figure 4 shows the reconstructed images for an undersampling ratio of 64, corresponding to only 8 elements used for imaging. Without *a priori* information, the targets are unrecognizable whereas the locations and borders of all features are faithfully rendered for the three algorithms. The high undersampling for this configuration introduces visible errors, however, as evidenced by considerable "graininess" demonstrated in the constrained backprojection image.

Limited View Problem

One important class of imaging scenarios involves limited data sets that consist of consecutive elements comprising only a portion of the total measurement surface. For examples, traditional ultrasound linear arrays can be used for tomographic imaging with rotation of the sample and/or transducer in a few discrete steps. High temporal resolution can be achieved without mechanical scanning but the limited angular view of the transducer surface produces severe distortions that can prevent location of critical features of interest[12]. The ability of the algorithms to improve these limited view problems was evaluated by considering a transducer with a 90° view. Figure 5 depicts the images and reconstructed mean values for the circular target. Without *a priori* information, the target is severely distorted with the higher aspect ratio features oriented away from the transducer unrecognizable. The constrained backprojection algorithm correct defines the features and edges, but retains some artifacts of the limited view. The

algorithms employing estimated data perform well, preserving uniformity and feature shape.

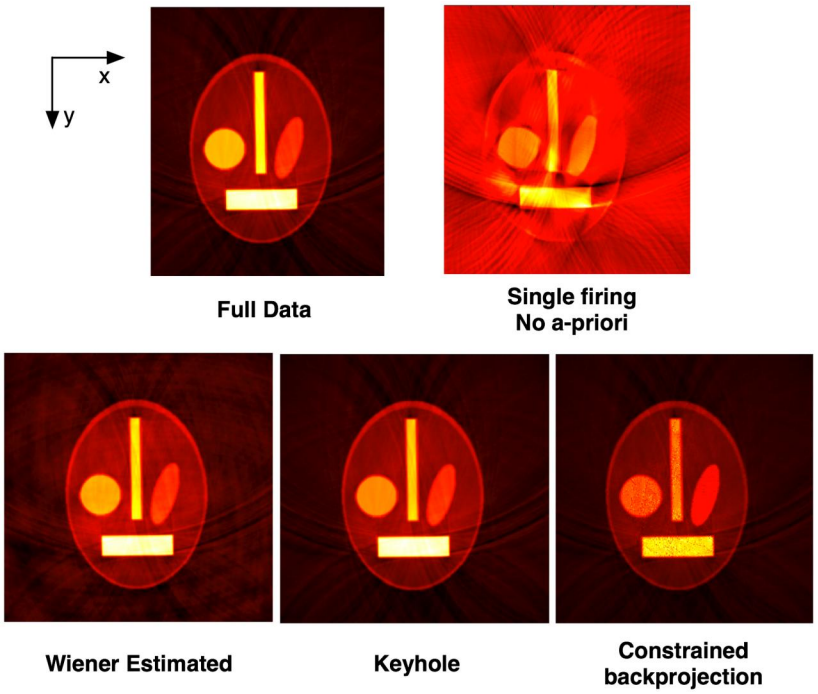

Figure 3. Image comparison for ellipse-square phantom.

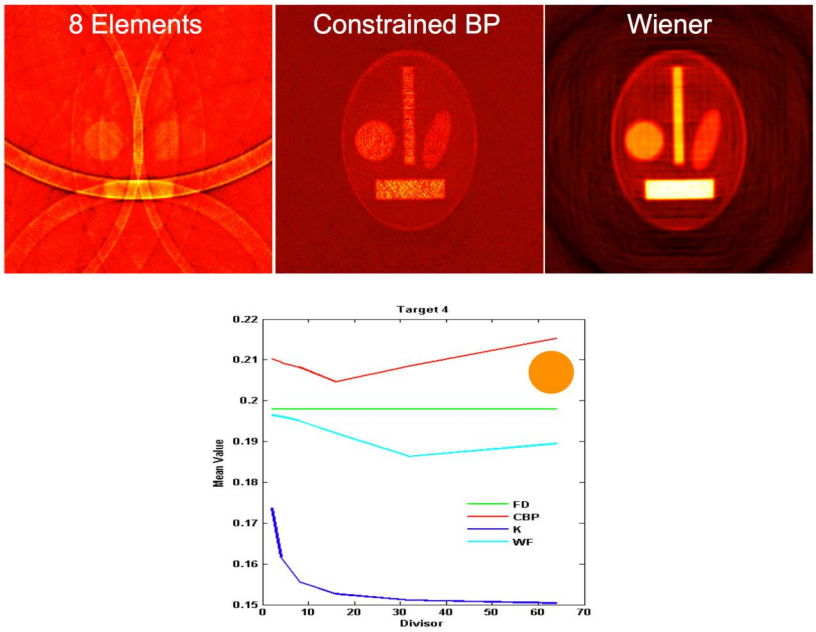

Figure 4. Reconstructions for various undersampling ratios. The images correspond to an undersampling of 64, corresponding to 8 elements.

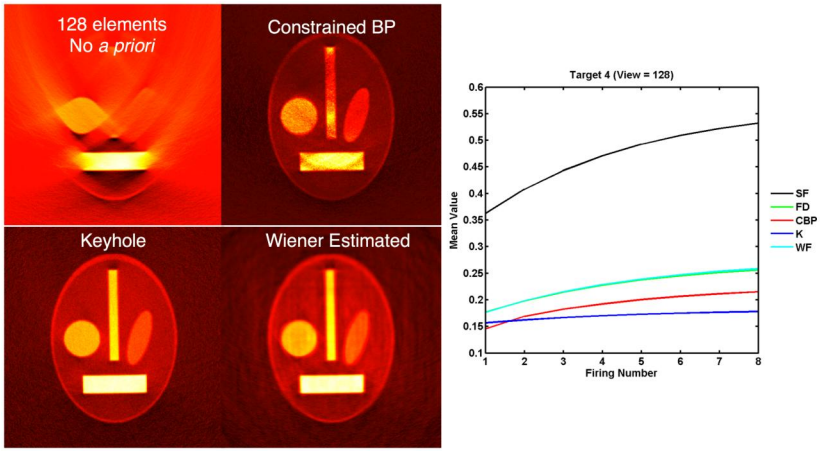

Figure 5. Images and mean value plots for ellipse-square phantom with 128 element, 90-degree view.

4. PHANTOM AND *IN VIVO* STUDIES

The performance of the algorithms with real data and noise was investigated using both phantom and animal imaging. Clear polyethylene tubing with an inner diameter of 1 mm was twisted into a looping pretzel configuration and a diluted india ink solution flowed through the tubing using a syringe over the time course of a few seconds. Because of the large changes in the absorption profile (no ink to high absorption), a continuously updating reference was progressively formed from the data set. Figure 6(a) depicts images of at time t=4.5 seconds from a larger data set of 10 seconds. To the authors' knowledge, the frame rate of 8 frames/second represents the fastest tomographic imaging speed obtained to date, corresponding to a time resolution of 130 milliseconds.

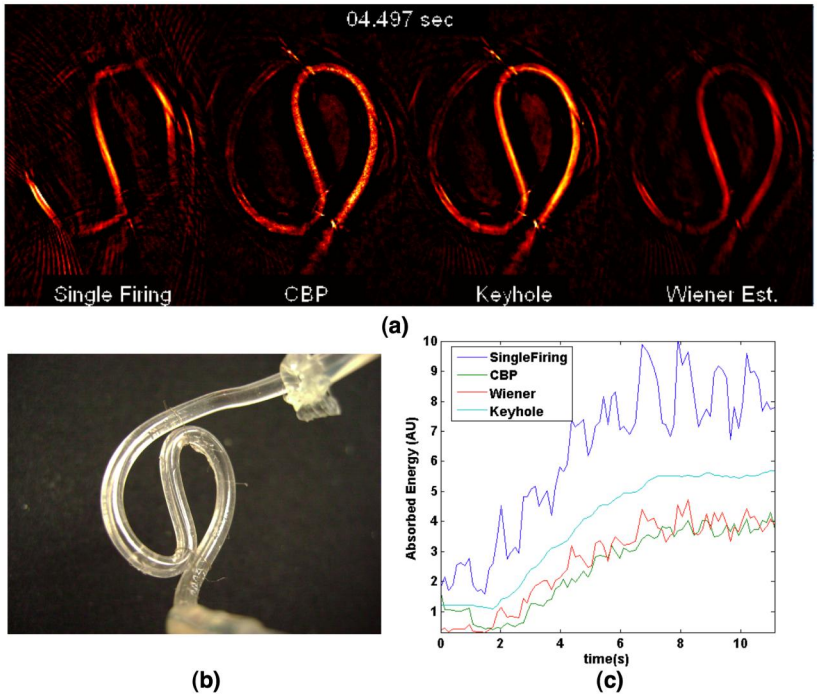

Figure 6. Comparison of images of dynamic ink flow through tubing.

Without *a priori* information, sections of the tubing are not visible and adjacent sections exhibit limited-view artifacts. In contrast, all of the *a priori*-based algorithms image all portions of the tubing well. As with the simulation results, some "salt-and-pepper" graininess was present in the constrained backprojection algorithm images. Nevertheless, as illustrated in Figure 6(c), the algorithms captured the time course of the flow (here represented as the mean value over the whole image).

As a more stringent test, the algorithms were tested on *in vivo* imaging of 20-g, white CD-1 mice. The mice were anaesthetized with a continous flow of 2% isoflurane and their brain vasculature imaged under a protocol approved by the University of Connecticut Institutional Animal Use and Care Committee. Figure 7 depicts side-by-side comparisons of images obtained from one frame of a 10-second sequence. Because of the more complex orientation and aspect-ratio of the features, the images without *a priori* consideration exhibit severe warping of the vasculature features which are faithfully preserved with the algorithms taking the *a priori* data into account.

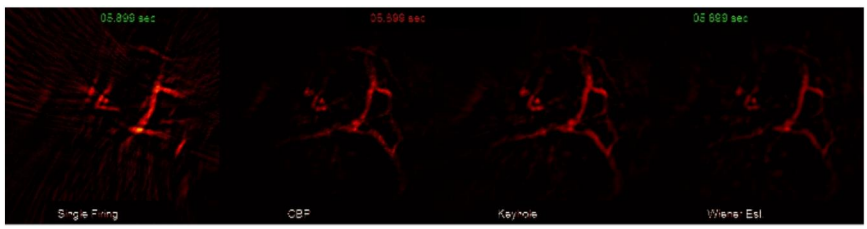

Figure 7. Comparison of images for in vivo mouse brain imaging.

5. DISCUSSION AND CONCLUSION

We have presented results of preliminary investigations of three algorithms using a priori information to simultaneously improve time and spatial resolution for systems constrained by multiplexing or mechanical scanning. Each technique is fast and direct, involving at most application of a frequency-domain filter, so that real-time imaging limited only by the laser repetition rate is possible. The underlying assumption of all the methods is that deviations from the a priori data set are small. In situations for which variations can be larger, a high-quality rolling reference can be applied using data accumulated continuously throughout the imaging.

Further improvements to the quantitative accuracy, particularly for fast and very heterogeneous changes, could potentially be obtained using iterative methods such as those based upon compressed sensing[1, 2, 4]. Iterative approaches, however, require knowledge of the forward photoacoustic propagation model which is not only complex to determine with transducer focusing, but also generally requires three-dimensional knowledge of the absorption profile. The methods outlined in this paper, however, only involve measured data without complications of an assumed propagation and imaging model. This advantage, coupled with the speed possible without iteration, offers the potential for real-time imaging and simultaneous display for fast transient phenomena.

Each of the presented techniques has their own advantages and disadvantages that suit specific imaging situations. Constrained backprojection requires the least image processing time (small number of projections) but has been found to most sensitive to reference data SNR and produces images with some coarse-grained variations. The keyhole method offers the most robust imaging but is appropriate only for low undersampling ratios with fixed references and exhibits a small time lag for rolling composite references. Wiener estimation is very responsive to fast dynamic changes and can produce high-quality images due to the complete data set that reduces artifacts and noise background. Attention to implementation details such as the noise model and handling of low-spectral components, however, is critical to preventing introduction of deconvolution artifacts.

As our results have demonstrated, the substantial improvement in feature definition and spatial resolution possible with each of the *a priori*-based techniques can facilitate realization of the long-sought promise of dynamic functional photoacoustic tomographic imaging.

6. ACKNOWLEDGMENTS

We acknowledge partial support from NIH grants NIH R01EB002136 and the Patrick and Catherine Weldon Donaghue Research Foundation. The authors can be contacted at via e-mail at zhu@engr.uconn.edu.

7. REFERENCES

[1]G. H. Chen, J. Tang, & S. Leng, "Prior image constrained compressed sensing (PICCS): A method to accurately reconstruct dynamic CT images from highly undersampled projection data sets," MEDICAL PHYSICS **35(2),** 660-663 (2008).

[2]U. Gamper, P. Boesiger, & S. Kozerke, "Compressed sensing in dynamic MRI," Magnetic resonance in medicine : official journal of the Society of Magnetic Resonance in Medicine / Society of Magnetic Resonance in Medicine **59(2),** 365-373 (2008).

[3]R. A. Jones, O. Haraldseth, T. B. Muller, & P. A. Rinck, "K-space substitution: A novel dynamic imaging technique," Magn Reson Med **29(6)**, 830-834 (1993).

[4]M. Lustig, D. Donoho, & J. M. Pauly, "Sparse MRI: The application of compressed sensing for rapid MR imaging," Magnetic resonance in medicine : official journal of the Society of Magnetic Resonance in Medicine / Society of Magnetic Resonance in Medicine **58(6),** 1182-1195 (2007).

[5]C. Mistretta, O. Wieben, J. Velikina, W. Block, J. Perry, Y. Wu et al., "Highly constrained backprojection for time-resolved MRI," Magn. Reson. Med. **55(1),** 30-40 (2005).

[6]Y. Xu, L. V. Wang, G. Ambartsoumian, & P. Kuchment, "Reconstructions in limited-view thermoacoustic tomography," Med Phys **31(4),** 724-733 (2004).

[7]Gonzales, R., Woods, R., & Eddins, S., [Digital Image Processing Using Matlab], Prentice Hall, (2003).

[8]G. J. Diebold, T. Sun, & M. I. Khan, "Photoacoustic monopole radiation in one, two, and three dimensions," Physical Review Letters **67(24),** 3384-3387 (1991).

[9]J. Gamelin, A. Aguirre, A. Maurudis, F. Huang, D. Castillo, L. V. Wang et al., "Curved array photoacoustic tomographic system for small animal imaging," J Biomed Opt **13(2),** 024007 (2008).

[10]K. P. Kostli & P. C. Beard, "Two-dimensional photoacoustic imaging by use of fourier-transform image reconstruction and a detector with an anisotropic response," Appl Opt **42(10),** 1899-1908 (2003).

[11]P. Burgholzer, J. Bauer-Marschallinger, & H. Grün, "BP algorithms for photoacoustic tomography with linear detectors," Inverse Problems **23(6)**, S65-80 (2007).

[12]X. Yang, A. Maurudis, J. Gamelin, Q. Zhu, & L. H. V. Wang, "Three-dimensional imaging of small animal brain using a curved array," Appl. Opt., in press**.**